JOURNAL OF SCIENCE
SAKARYA UNIVERSITY

Sakarya University Journal of Science

ISSN 1301-4048 | e-ISSN 2147-835X | Period Bimonthly | Founded: 1997 | Publisher Sakarya University | http://www.saujs.sakarya.edu.tr/

Title: Optimized Analytical Solution of Platform Panel Radiative Area Dimensioning of Geostationary Communications Satellites: A Practical Approach

Authors: Murat Bulut, Nedim Sözbir
Recieved: 2019-03-29 21:45:14

Accepted: 2019-06-17 12:53:04

Article Type: Research Article
Volume: 23
Issue: 5
Month: October
Year: 2019
Pages: 986-992

How to cite
Murat Bulut, Nedim Sözbir; (2019), Optimized Analytical Solution of Platform Panel Radiative Area Dimensioning of Geostationary Communications Satellites: A Practical Approach. Sakarya University Journal of Science, 23(5), 986-992, DOI: 10.16984/saufenbilder.546894
Access link
http://www.saujs.sakarya.edu.tr/issue/44066/546894

Sakarya University Journal of Science 23(5), 986-992, 2019

Optimized Analytical Solution of Platform Panel Radiative Area Dimensioning of Geostationary Communications Satellites: A Practical Approach

Murat Bulut*[1], Nedim Sözbir[1,2,3]

Abstract

Determining radiative areas of geostationary satellite are one of the challenging tasks for satellite thermal engineers at the early stage of the project. Radiative areas of geostationary communication satellite for the payload and platform panels are determined based on worst hot case (end-of-life). After calculation of radiative areas, it needs to be optimized according to worst hot and cold scenario at sun acquisition mode, orbit raising mode and geostationary orbit. Authors, in this study, optimized geostationary satellite platform panel. The radiator's dimensions were calculated and then optimized based on sun acquisition mode, orbit raising mode and geostationary orbit. Determining radiative areas of GEO satellite is important task. Radiative areas always are determined based on hot case condition at EOL. On the other hand, these radiative areas needs to be optimized according SAM, ORM, and GEO scenario. Calculated radiative areas both the north panel and the south panel was 1 m^2. Radiative areas were studied at +/-10% m^2. It was seen from the analytical results that the surface temperature of the platform panel areas were between -48.5 ºC at 1.1 m^2 of radiative area and 37.7 ºC at 0.9 m^2 of radiative area.

Keywords: geostationary earth orbit satellite, thermal analysis, launcher, solar array

1. INTRODUCTION

The thermal control system (TCS) of a satellite is to maintain temperature of the electronic components of a satellite within acceptable limits during service life. TCS is divided into three parts which are thermal design, analysis, and test. Based on the results of thermal analysis, thermal design is optimized and verified by the thermal balance test [1]. Passive and active thermal control techniques are used during TCS. Passive thermal control technique includes in heat pipe (HP), optical solar reflector (OSR), and paintings. Active thermal control technique includes in

* Corresponding Author: bulut44@gmail.com
[1] Turksat Satellite Communication Cable TV and Operations Joint Stock Co., Satellite Programs Directorate, Golbasi, Ankara, Turkey. ORCID: 0000-0002-9024-7722
[2] Sakarya University, Mechanical Engineering Department, Esentepe, Sakarya, Turkey. ORCID:0000-0003-4633-2521
[3] Tübitak MAM, Gebze, Kocaeli, Turkey. ORCID:0000-0003-4633-2521

heaters and thermistors. Thermocouples are used during the thermal test.

Preliminary design review (PDR) and critical design review (CDR) are two main milestones of the satellite project during thermal design and thermal analysis. At PDR phase, radiative areas of the satellite are calculated and then at CDR phase, radiative areas are finalized. Satellite thermal engineers always face the challenge of determining radiative areas at the stage of PDR and CDR phase.

Radiator system optimization is very common subject that many researches have been published numerous studies [2-11] but there is no paper established in optimized platform panel radiative area of three-axis stabilized geostationary communications satellites.

Curran and Lam [2] studied a mathematical model of the spacecraft that had embedded heat pipes in order to optimize radiator area according to payload heat rejection. They calculated the minimum weight configuration based on radiator surface parameters, heat pipe spacing, panel thermal conductives and facesheet thickness [2]. Sam and Deng [3] presented optimization of radiator area of geostationary communications satellite. Optimization of four radiator areas was done by using SINDA/FLUINT commercial software. Analysis results showed that reduction of the total weight was 5.87 kg. Comparing between initial approach and final approach, the weight saved was 1.5 kg. Arslanturk [4] presented the correlation equations to find the optimum dimensions of space radiators in order to maximize the heat transfer per unit radiator mass. Cockfield [5] studied on structural optimization of a radiator area. Kelly et al. [6] studied optimization of a heat pipe radiator area of spacecraft that had high power TWTAs. They developed a detailed analytical model of the radiator to evaluate thermal performance under worst-case environmental and operational conditions. Muraoka et al. [7] developed a simplified thermal model to calculate the optimum radiator/solar absorber areas and then the results of a simplified thermal model were implemented in a detailed thermal model. Their main study was to reduce computational time and to optimize the radiator areas [7]. Hull et al. [8] presented the development of detailed analysis tool to design radiator area. Kim et al. [9] presented two radiator design optimization methods based on node division of the thermal model. An integrated analysis combining an optimization algorithm with thermal analysis was used at the first method. A radiator node stepwise was added based on a temperature sensitivity at the second method. Kim et al. [10] studied the optimization of a spacecraft radiator. The aim of the study was both enhancing the thermal performance and reducing mass of the spacecraft. Honeycomb core, the distance between heat pipes, facesheet thickness were three parameters during the optimization of the radiator areas. A strategy for a quick determination of the optimum configuration for radiators and solar absorbers in a spacecraft thermal design was presented Muraoka et al. [7]. The aim of the study was to maximize temperature margins and minimize heater power consumption. Hung and Deng [11] presented thermal design and optimization of a heat pipe raditor. A heat pipe radiator consisted of surface mounted heat pipe and embedded heat pipe. After sizing optimization of mounted and embedded heat pipes, minimum weight of the radiator was obtained.

In this study, radiative areas of the platform panels were optimized by analytical solution.

2. SATELLITE DESIGN DESCRIPTION

Figure 1 shows geostationary communication satellite which consists of gregorian antenna, deployable antenna, solar array, main structure and apogee boost motor (ABM) as the main parts. North and south panel outer surface areas are covered by multi layer insulation (MLI) excep radiative areas, which are cover with optical solar reflector (OSR). MLI contain multi-layers of metalized mylar or kapton with little contact between each layer (to reduce conduction transfer). MLI has small emittance and absorptance [12]. OSR reflect the sun, but dissipate the heat through surfaces to which they are attached. The optical solar reflector has lower absorptivity value and higher emissivity value. The ratio of absorptivity/emissivity is low.

Therefore, OSR is material to use in space environment as thermal control system hardware [13]. Solar arrays are located at north and south panels in +y and -y directions. Deployable antennas are located at east and west panels in +x and –x directions. ABM is located zenith side in -z direction. Gregorian antenna is located on nadir panel in +z direction.

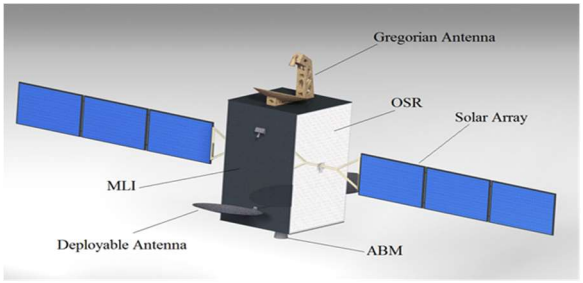

Figure 1. Geostationary communication satellite at GEO

The AOCS has three modes of operation which are sun acquisition mode (SAM), Inertial Attitude Acquisition Mode (IAAM) and Orbit Raising Mode (ORM) during transfer orbit (TO). These modes may be entered automatically or manually by ground control. Figure 2 shows AOCS of the satellite with respect to three modes at TO. SAM brings the satellite from an arbitrary initial condition to a sun pointing attitude, i.e. the desired principal axis is pointed to the sun and the satellite is to rotate around the sunline with a constant rate [14]. At ORM, the solar arrays are folded against two opposite sides of the satellite body which is spinning while the satellite is at SAM and ORM. Figure 3 shows the satellite at ORM and SAM.

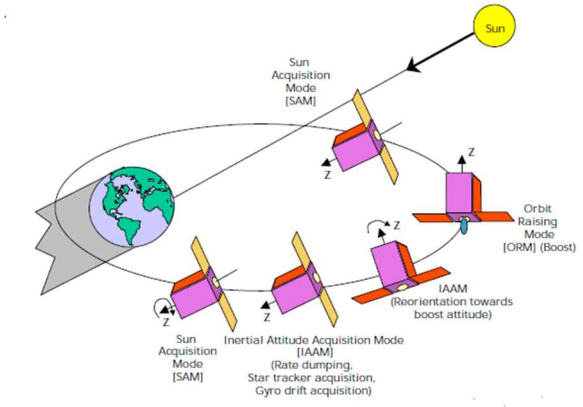

Figure 2. AOCS modes of the satellite at transfer orbit [15]

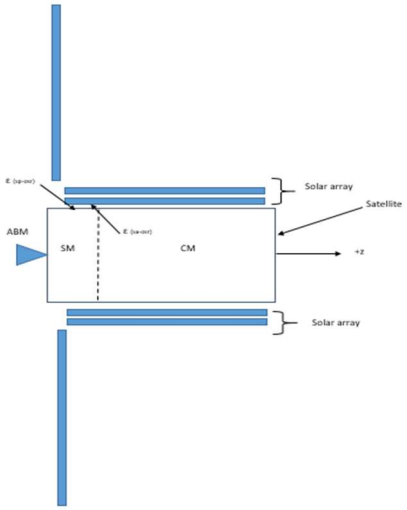

Figure 3. The satellite at ORM and SAM

3. THERMAL ANALYSIS DESCRIPTION

The main goals of TCS is to make sure that the internal components of the satellite remain within their acceptable temperature during the worst hot and cold conditions during service life. A steady-state thermal analysis and a transient thermal analysis are two types of thermal analysis[16-18]. A steady state thermal analysis determines the temperature distribution and other thermal quantities under conditions that a period of time can be ignored [17]. A transient thermal analysis determines the temperature distribution and other thermal quantities under conditions that vary over a period of time [17].

Energy balance for satellite is written as follows in equation (1) and (2).

$$Q_{in}=Q_{out} \tag{1}$$

$$Q_S+Q_A+Q_E+Q_d=Q_{Rad-S} \tag{2}$$

The left side equation (1); Q_S is environmental heat load from solar, Q_A is environmental heat load from albedo, Q_E is environmental heat load from Earth and Q_d is heat dissipition from electronic device. Heat load received by spacecraft (Q_{Rad-S}) is shown on the right side equation.

Equation (3) shows the heat balance between the radiator and the space environment in steady state [19].

$$(A_S q_S + A_A q_A)\alpha + A_E q_E \varepsilon + Q_d = A_{surface}\sigma T^4 \varepsilon \quad (3)$$

where A_S is the projected areas of solar, A_A is the projected area of albedo, A_E is the projected area of Earth, the satellite radiator area is $A_{surface}$. q_S, q_A and q_E are sun flux, albedo flux and Earth flux, respectively. α is absorptivity. ε is emissivity. σ is Stefan-Boltzmann constant σ is $5.699*10^{-8}$ W/m^2K^4 . T is temperature.

In Figure 4, radiator energy balance is also represented. Radiator areas of the satellite reject heat by infrared (IR) radiation. The radiating power depends on the surface emmisivity values and temperature of radiator surface area. Radiataive areas were covered by OSR material in order to reject heat from the satellite. Figure 4 shows radiator energy balance.

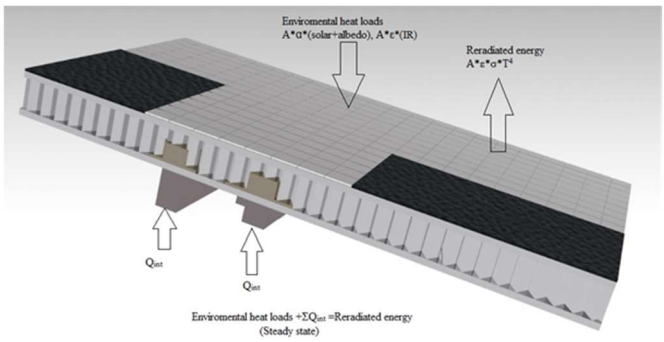

Figure 4. Radiator energy balance

Radiative area is optimized by using the following equation.

$$Q = A_{surface} * \sigma * \left[\left(\varepsilon_{SP\text{-}OSR} * \left(T_{OSR}^4 - T_{space}^4\right) + \varepsilon_{SA} * \left(T_{OSR}^4 - T_{SA}^4\right)\right)\right] \quad (4)$$

Q is the total heat loads comes from components and external heat. $A_{surface}$ is the radiative area. $\varepsilon_{SP\text{-}OSR}$ is emissivity of OSR at structural panel. ε_{SA} is emissivity of solar array backside. T_{OSR} is the temperature of OSR at platform panel. T_{space} is the temperature of space environment which is taken as 4 °K. T_{SA} is the temperature of solar array. $A_{surface}$ would be assumed and T_{OSR} would be calculated. The respresentation of $\varepsilon_{SP\text{-}OSR}$ and $\varepsilon_{SA}$is shown in Figure 3.

3.1. Thermal Analysis Input

In this study, the values and properties are taken as follows. At the beginning of life (BOL), The solar absorptivity of the OSR was taken approximately 0.11. The emissivity of the OSR ($\varepsilon_{SP\text{-}OSR}$) and the emissivity of solar array back side (ε_{SA}) would be approximately 0.84 and 0.42, respectively at BOL. The space temperature was taken at 4 °K. The solar array temperature of 20 °C at SAM and 60 °C at ORM are selected for the steady state thermal analysis. The intensity of solar radiation is 1418 W/m^2. The internally generated heat dissipation by components is shown in Table 1.

Table 1. Platform panel heat dissipation

Mode	Case	North panel (W)	South panel (W)
SAM	Cold	93.7	127.1
ORM	Cold	73.2	133.3
	Hot	73.2	133.3
GEO	Cold	189.3	123.7

The radiator's dimensions were determined considering cold scenario at sun acquisition mode (SAM), hot and cold scenario at orbit raising mode (ORM) and cold scenario at geostationary orbit (GEO). Four cases are considered during the analytical solution. Table 1 shows the list of the cases with respect to heat dissipation values. They are three cold cases (SAM, ORM and GEO) and one hot case (ORM). The mission, the orientation, surface properties and the size of the satellite are key parameters to determine the external head loads that are receive from the satellite. Knowing these parameters, the absolute worst hot and cold case conditions are determined [20]. The satellite is in sunlight during hot case conditions. The satellite does not see the Sun during col case condition.

4. RESULTS AND DISCUSSIONS

A steady state analysis was used at SAM, ORM, and GEO as the initial thermal analysis. Table 2

and Table 3 shows OSR area vs OSR temperature at north and south platform panel.

Table 2. OSR area vs OSR temperature at north platform panel

	North panel			
Mode	**SAM**	**ORM**		**GEO**
Case	**Cold**	**Hot**	**Cold**	**Cold**
SA temperature	20°C	60°C	60°C	60°C
Solar flux (W/m²)	0	1418	0	0
Dissipation (W)	93.7	73.2	73.2	189.3
OSR area (m²)	OSR temperature (°C)			
0.9	-2.43	20.81	-39.84	-15.36
0.92	-3.23	20.32	-40.82	-16.78
0.94	-4.01	19.85	-41.77	-18.15
0.96	-4.76	19.4	-42.69	-19.49
0.98	-5.48	18.97	-43.59	-20.79
1	-6.18	18.55	-44.46	-22.06
1.01	-6.52	18.34	-44.88	-22.69
1.02	-6.86	18.14	-45.3	-23.3
1.04	-7.52	17.75	-46.12	-24.51
1.06	-8.15	17.37	-46.92	-25.7
1.08	-8.77	17	-47.7	-26.85
1.1	-9.37	16.65	-48.45	-27.98

In Table 2, at 0.9 m^2 of radiative areas, the OSR temperatures at north panel is between -39.84 ºC and 20.81 ºC. The coldest temperature is at ORM (cold case). The hottest temperature is at ORM (hot case). The temperature difference between the coldest temperature and the hottest temperature is 60.61 ºC. At 1.1 m^2 of radiative areas, the OSR temperatures at north panel varies between -48.45 ºC and 16.65 ºC. The coldest temperature is at ORM (cold case). The hottest temperature is at ORM (hot case). The temperature difference between the coldest temperature and the hottest temperature is 55 ºC. OSR temperatures at ORM (cold case) for north panel varies -39.8 ºC (0.9 m^2) and -48.5 (1.1 m^2). The temperatures difference is 8.7 ºC.

Table 3. OSR area vs OSR temperature at south platform panel

	South panel			
Mode	**SAM**	**ORM**		**GEO**
Case	**Cold**	**Hot**	**Cold**	**Cold**
SA temperature	20°C	60°C	60°C	60°C
Solar flux (W/m²)	0	1418	0	0
Dissipation (W)	127.1	133.3	133.3	123.7
OSR area (m²)				
0.9	9.8	37.7	-9.49	-17.29
0.92	8.85	36.95	-10.73	-18.69
0.94	7.93	36.22	-11.93	-20.06
0.96	7.04	35.52	-13.1	-21.39
0.98	6.17	34.84	-14.23	-22.68
1	5.34	34.19	-15.34	-23.94
1.01	4.93	33.87	-15.88	-24.56
1.02	4.53	33.56	-16.41	-25.17
1.04	3.74	32.95	-17.46	-26.37
1.06	2.98	32.35	-18.48	-27.55
1.08	2.24	31.78	-19.47	-28.69
1.1	1.52	31.22	-20.44	-29.81

In Table 3, at 0.9 m^2 of radiative areas, the OSR temperatures at south panel is between -17.29 ºC and 37.7 ºC. The coldest temperature is at GEO (cold case). The hottest temperature is at ORM (hot case). The temperature difference between the coldest temperature and the hottest temperature is 54.99 ºC. At 1.1 m^2 of radiative areas, the OSR temperatures at south panel is between -29.81 ºC and 31.22 ºC. The coldest temperature is at ORM (cold case). The hottest temperature is at ORM (hot case). The temperature difference between the coldest temperature and the hottest temperature is 61.03 ºC. OSR temperatures at ORM (hot case) for south panel varies 37.7 ºC (0.9 m^2) and 31.22 ºC (1.1 m^2). The temperatures difference is 6.58 ºC.

5. CONCLUSIONS

Determining radiative areas of GEO satellite is important task at early stage of the project. Radiative areas always are determined based on hot case condition at EOL. On the other hand, these radiative areas needs to be optimized according SAM, ORM, and GEO scenario. In this

study, the analytical solution was carried out to optimize the radiative areas of payload panels (the north and the south panels) that were 1 m^2 for each panel. Radiative areas were studied at +/- 10% m^2. Radiative areas of north and south panels from 0.9 m^2 to 1.1 m^2 were studied.

The results showed that OSR temperature of the panels depended on SAM, ORM, and GEO scenario. Increasing the radiative areas from 0.9 m^2 to 1.1 m^2 for the north panel, the coldest temperature decreased from -39.84 ^oC to -48.45 ^oC. The hottest temperature decreased from 20.81 ^oC to 16.65 ^oC. Increasing the radiative areas from 0.9 m^2 to 1.1 m^2 for the south panel, the coldest temperature decreased from -17.29 ^oC to -29.81 ^oC. The hottest temperature decreased from 37.7 ^oC to 31.22 ^oC.

It was seen from the results that at north panel OSR areas (1.1 m^2), the lowest temperature occurred as -48.45 ^oC. That means that north panel needed more heating power in order to maintain equipment within acceptable temperature limit. At south panel OSR areas (0.9 m^2), the highest temperature occurred as 37.7 ^oC.

Based on the above results, satellite thermal engineers focus on the optimization of radiative areas based on radiative areas availability and heating power availability in the satellite.

6. REFERENCES

[1] L. Yang, Q. Li, L. Kong, S. Gu and L. Zhang, "Quasi-all-passive thermal control system design and on-orbit validation of Luojia 1-01 satellite," *Sensors,* vol. 19, pp. 827-18, 2019.

[2] D. Curran and T.T. Lam, "Weight optimization for honeycomb radiators with embedded heat pipes," *Journal of Spacecraft and Rockets,* vol. 33, pp. 822-828, 1996.

[3] K.F.C.H. Sam and Z. Deng, "Optimization of a space based radiator, " *Applied Thermal Engineering*, vol.31, pp. 2312-2320, 2011.

[4] C. Arslanturk, "Optimum design of space radiators with temperature-dependent thermal conductivity," *Applied Thermal Engineering,* vol. 26, no. 17-18, pp. 1149-1157, 2006.

[5] R.D. Cockfield, "Structural optimization of a space radiator," *Journal of Spacecraft and Rockets,* vol. 5, no. 10, pp. 1240-1241, 1968.

[6] W.H. Kelly and Jr. J.H. Reisenweber 1982, "Optimization of a radiator heat pipe radiator for spacecraft high-power TWTAs," *Advances in Heat Pipe Technology, Proceedings of the IVth International Heat Pipe Conference*, London, UK, 1981.

[7] I. Muraoka, R.L. Galski, F.L De Sousa and F.M. Ramos, "Stochastic spacecraft thermal design optimization with low computational cost," *Journal of Spacecraft and Rockets,* vol. 43, no. 6, 2006.

[8] P.V. Hull, M. Tinker, M. SanSoucie, K. Kittredge, Thermal analysis and shape optimization of an in-space radiator using genetic algorithms, *AIP Conference Proceedings 813* (81), 2006.

[9] H.K. Kim, S. Choi, S.O. Park and K.H. Lee, "Node-based spacecraft radiator design optimization," *Advances in Space Research,* vol. 55, no. 5, pp. 1445-1469, 2015.

[10] T. Y. Kim, S. Chang and S. S. Young, "Optimizing the design of space radiators for thermal performance and mass reduction," *Journal of Aerospace Engineering*, vol. 30, no. 3, 04016090-1-04016090-6, 2017.

[11] A.D. Willams and S.E. Palo ,"Issues and Implications of the Thermal Control Systems on the ' six day spacecraft', " *in: 4th Responsive Space Conference, RS4-2006-6001*, Los Angeles, California, USA, 2006.

[12] B. Pattan, Satellite Systems Principles and Technologies, New York, NY, Van Nostrand Reinhold; 1993, ISBN-13: 978-0442013578

[13] M. G. Boato, E.C. Garcia, M.B. Dos Santos and A.F. Beloto, "Assembly and Testing of a Thermal Control Component Developed in Brazil," *Journal of Aerospace Technology and Management,* vol.9. no.2, 2017.

[14] D.B. DeBra and E. Gottzein "Automatic Control in Aerospace 1992," *the 12th IFAC Symposium,* Ottobrunn, Germany, 1992.

[15] Alcatel Alenia Space, Space Engineering & Operations University, AOCS Attitude and Orbit Control Subsystem Spacecraft Introduction Session, Ref: 200203304L Issue 1, 2005.

[16] M. Bulut and N. Sozbir "Analytical investigation of a nanosatellite panel surface temperatures for different altitudes and panel combinations," *Applied Thermal Engineering*, vol. 75, pp. 1076-1083, 2015.

[17] M. Bulut and N. Sozbir " Thermal Design of a Geostationary Orbit Communications Satellite, Electronic World, Pages: 28-32, August 2016.

[18] M. Bulut, "Thermal simulation software based on excel for spacecraft applications," *Selcuk University Journal of Engineering ,Science and Technology*, vol. 6, no. 7, pp. 596-600, 2018.

[19] M. Bulut and N. Sozbir, "Heat rejection capability for geostationary satellites," *9th Ankara International Aerospace Conference (AIAC 2017)*, METU, Ankara, Turkey, 2017.

[20] K.F.C.H. Sam and D. Zhongmin, "Optimization of a space based radiator," *Applied Thermal Engineering*, vol. 31, pp. 2312-2320, 2011.